

Published in final edited form as:

Cell Metab. 2011 August 3; 14(2): 219–230. doi:10.1016/j.cmet.2011.06.010.

Disrupting the CH1 domain structure in the acetyltransferases CBP and p300 results in lean mice with increased metabolic control

David C. Bedford¹, Lawryn H. Kasper¹, Ruoning Wang², Yunchao Chang¹, Douglas R. Green², and Paul K. Brindle^{1,*}

¹Department of Biochemistry, St. Jude Children's Research Hospital, Memphis, TN 38105, USA

²Department of Immunology, St. Jude Children's Research Hospital, Memphis, TN 38105, USA

SUMMARY

Opposing activities of acetyltransferases and deacetylases help regulate energy balance. Mice heterozygous for the acetyltransferase CREB binding protein (CBP) are lean and insulin-sensitized but how CBP regulates energy homeostasis is unclear. In one model, the main CBP interaction with the glucagon-responsive factor CREB is not limiting for liver gluconeogenesis, whereas a second model posits that Ser436 in the CH1 (TAZ1) domain of CBP is required for insulin and the anti-diabetic drug metformin to inhibit CREB-mediated liver gluconeogenesis. Here we show that conditional knockout of *CBP* in liver does not decrease fasting blood glucose or gluconeogenic gene expression, consistent with the first model. However, mice where the CBP CH1 domain structure is disrupted by deleting residues 342-393 (Δ CH1) are lean and insulin-sensitized, as are p300 Δ CH1 mutants. *CBP Δ CH1/ACH1* mice remain metformin responsive. An intact CH1 domain is thus necessary for normal energy storage, but not for the blood glucose-lowering actions of insulin and metformin.

INTRODUCTION

Energy homeostasis, defined as the balance between energy intake, storage, and expenditure, is regulated in part by energy-sensing sirtuin protein deacetylases (Yu and Auwerx, 2009). Less well understood in the control of energy balance are the roles of protein or histone lysine acetyltransferases (HATs or KATs), which acetylate many metabolic enzymes (Zhao et al., 2010), as well as targets of sirtuin-mediated deacetylation (Hirschey et al., 2010). While it is assumed that the enzymatic activities of HATs are critical for energy balance, the roles of their distinct domains that impart regulatory specificity by binding to transcription factors and other proteins are less clear.

CBP (*Crebbp*) and the closely related p300 (*Ep300*) comprise the KAT3 family of HAT transcriptional coactivators (Allis et al., 2007). Most of the conserved regions of CBP and p300, including those harboring acetyltransferase activity, have little sequence similarity with other HAT families, suggesting that CBP/p300 have unique functions (Bedford et al., 2010; Marmorstein, 2001). Indeed, CBP and p300 are required for normal development, as loss of either one results in early embryonic lethality in mice (Tanaka et al., 1997b; Yao et al., 1998).

*Corresponding author Department of Biochemistry St. Jude Children's Research Hospital 262 Danny Thomas Place, Memphis, TN 38105 Telephone: 901-595-2522 Fax: 901-525-8025 paul.brindle@stjude.org .

The authors do not have any conflicts of interest to declare.

Studies of non-lethal mutants have been instructive in determining the role of CBP in later development and physiology. Mice heterozygous for a *CBP* null mutation are growth retarded, as are those heterozygous for an allele that produces a truncated form of CBP (Kung et al., 2000; Oike et al., 1999). The latter mutant has been the more extensively characterized of the two, and it is lean (“lipodystrophic”) and more insulin sensitive than wild type controls, suggesting that CBP is an important regulator of energy homeostasis (Yamauchi et al., 2002). In this regard, CBP is modeled as central to the counter regulatory effects of glucagon and insulin on gene expression that is required for hepatic gluconeogenesis (He et al., 2009; Yamauchi et al., 2002; Zhou et al., 2004), a critical process for maintaining glucose homeostasis (Biddinger and Kahn, 2006).

During fasting, glucagon produced by the pancreas promotes hepatic glucose production by increasing intracellular cyclic AMP in the liver. Hepatic gluconeogenic gene transcription is stimulated via the recruitment of HAT (CBP/p300) and non-HAT (CRTC) coactivators to the cAMP-responsive transcription factor CREB that is bound to the promoters of target genes (Herzig et al., 2001; Koo et al., 2005). However, mice homozygous for a mutation in CBP that ablates the interaction of CREB and the KIX domain of CBP (Kasper et al., 2002; Xu et al., 2007) have fasting blood glucose levels and hepatic gluconeogenic gene expression that are similar to controls (Koo et al., 2005). This suggests that other domains of CBP besides KIX may be critical for glucose regulation, or that p300 (or the non-HAT CRTC2) can compensate for KIX mutant CBP. Conversely, mice with a serine to alanine mutation in the CH1 domain of CBP (Ser436Ala) display increased hepatic gluconeogenic gene expression, increased fasting blood glucose, and are resistant to the hypoglycemia-inducing effects of insulin and metformin (He et al., 2009; Zhou et al., 2004). Since p300 lacks an equivalent serine residue in CH1 (Figure 3A), those studies suggest that CBP has unique insulin- and metformin-responsive properties. Thus, the role of CBP in controlling liver gluconeogenesis is unresolved.

In this study, we inactivated CBP in the liver to further clarify these two models for hepatic gluconeogenesis. Consistent with earlier findings using CBP KIX domain mutant mice, we found that hepatic CBP does not appear to be limiting for maintaining blood glucose levels. To address whether the CH1 domain is needed for energy homeostasis and the glucose lowering effects of insulin and metformin, we used mice with germline knock-in deletion mutations in CBP and p300 that severely disrupt the structure of the domain. This revealed that the Δ CH1 mutation results in lean mice that respond normally to metformin, but have an enhanced insulin response. Together, our findings provide insight into how KAT3 acetyltransferases help maintain energy homeostasis, and suggest that the critical site of action for CBP in regulating glucose homeostasis is outside the liver.

RESULTS

Loss of CBP in the liver does not significantly reduce fasting blood glucose or hepatic gluconeogenic gene expression

Insulin- or metformin-dependent phosphorylation of CBP Ser436 is modeled to disrupt CBP binding to CREB-driven gluconeogenic genes in the liver, thereby repressing their expression and glucose production (He et al., 2009). A different model indicates that CBP is not limiting for liver gluconeogenesis because a mutation in its KIX domain that inhibits binding to CREB, does not significantly affect that process (Koo et al., 2005).

To resolve whether CBP in the liver is necessary for glucose homeostasis we injected *CBP^{flox/flox}* conditional knockout mice (Kang-Decker et al., 2004) with adeno-associated virus that expresses Cre recombinase from a liver-specific promoter (AAV-Cre). The mice were tested seven to eighteen days after AAV-Cre injection, depending on the assay (see

Experimental Procedures). We found that 16 and 6 hr fasting blood glucose levels were not significantly different between 5 month-old male wild type (WT) and *CBP^{fllox/fllox}* mice ($P>0.05$, Figures 1A, S1A), even though the mutants had markedly reduced levels of CBP in the liver (Figures 1B, S1B,C). A replicate experiment using different cohorts of female (6-9 month-old) and male (2-3 month-old) *CBP^{fllox/fllox}* mice seven days after AAV-Cre injection gave similar results for 16 hr fasting blood glucose ($P>0.05$, Figure S1D-E). Glucose tolerance tests (GTT, to measure the ability of the metabolic tissues to deal with a glucose load), and insulin tolerance tests (ITT, to determine the glucose lowering effect of bolus i.p. insulin injection) were also not significantly different between WT and *CBP^{fllox/fllox}* male mice ($P>0.05$, Figure S1F-I).

We then used qRT-PCR to measure mRNA in livers from fasted male and female mice. Expression of the gluconeogenic CREB-target genes *G6pc* (glucose-6-phosphatase), *Pck1* (PEPCK, phosphoenolpyruvate carboxykinase), and *Ppargc1a* (PGC-1 α , a master coregulator of hepatic gluconeogenic gene transcription) were not significantly different from WT animals ($P>0.05$, male data Figures 1C-E, S1M-O; female Figures S1J-L). CBP and p300 were expressed at comparable levels in WT liver (Figures S1P-R), and in CBP null livers we did not observe evidence for compensation by p300 or other CREB coactivators (i.e. increased expression of *p300*, *Crtc1* and *Crtc2* mRNAs) ($P>0.05$, Figures S1S-U). Also arguing against complete compensation for the loss of CBP, analysis of the CBP/p300-dependent genes *Ndr1* and *Ppp1r3c* [(Figure 1F,G; identified using CBP/p300 double-knockout (dKO) mouse embryonic fibroblasts (MEFs) (Kasper et al., 2010)] revealed they were also repressed in CBP null liver (Figure 1H,I). *Ndr1* was responsive to cAMP in MEFs, suggesting it is a CREB target (Figure 1F). Thus, there are CBP-dependent genes in the liver but they do not appear to be involved in glucose homeostasis. Together these results show that CBP in the liver is not limiting for gluconeogenic CREB target gene expression or glucose homeostasis. Moreover, since CBP deletion has no significant effect on these processes, it implies that phosphorylation of CBP Ser436 in the liver is also not critical.

Insulin does not rapidly inhibit the CREB:CBP complex, or expression of gluconeogenic genes in liver

The lack of a significant effect on glucose homeostasis when hepatic *CBP* was inactivated suggests that insulin does not act by inhibiting CBP binding at CREB target genes in the liver. To further test this idea, we examined whether insulin rapidly inhibits the CREB:CBP complex and CREB-dependent gluconeogenic gene expression. As expected, insulin i.p.-injected into WT mice that had been fasted overnight significantly lowered blood glucose after 30, 90, and 180 min (Figure 2A), and increased the phosphorylation of the insulin-responsive kinase AKT in the liver (Figure S2A). However, there was no significant effect upon *G6pc* or *Pck1* mRNA levels 90 and 180 min after insulin injection, whereas *Ppargc1a* mRNA tended to increase at 90 min albeit with more variability (Figure 2B-D). A different cohort of mice showed a similar pattern of gene expression after 30 and 90 min of insulin (Figure S2B-D). As a control for our ability to measure the metabolic regulation of genes in the liver, we examined mRNA levels 90 and 180 min after refeeding (which increases both insulin and satiety hormone release), and observed gene repression (Figure 2B-D). Thus distinct liver gene expression responses are seen when WT fasted mice are either injected with insulin or refeed, a phenomenon also observed by Lipina *et al.* (Lipina et al., 2005). Tilghman *et al.* similarly observed that insulin alone does not repress *Pck1* protein synthesis in fasted rats (Tilghman et al., 1974). Thus, activating the insulin pathway in the livers of fasted mice is not sufficient to inhibit the expression of *G6pc*, *Pck1* and *Ppargc1a*. Refeeding therefore appears to modulate the effect of insulin on hepatic gluconeogenic gene expression.

To further test the model of He *et al.* (He et al., 2009) where insulin alone disrupts the CREB:CBP complex at hepatic target genes, we performed qPCR chromatin immunoprecipitation (ChIP) on liver tissue from insulin-treated wild type mice. This showed that the occurrence of CBP, p300, and CRTC2 (TORC2) at CREB binding sites (CREs) in the *Pck1* promoter was not attenuated by insulin (Figure 2E). The CRTC2 ChIP signal actually increased moderately 30 min after insulin injection. Specificity of the CBP ChIP was confirmed using *CBP^{fllox/fllox}* mice injected with AAV-Cre (Figure 2F). CRTC2 and CBP ChIPs were further verified by using antigen-peptide-blocked antibodies (Figure S2E), and showing there was a lack of coactivator enrichment at a region ~20 kb upstream of the *Pck1* promoter CREB binding region (Figure S2F). It therefore appears that insulin alone does not rapidly inhibit the expression of *Pck1* or the binding of CBP at its promoter. Moreover, it seems unlikely that the insulin-dependent phosphorylation of CBP Ser436 in the liver is critical for repressing hepatic CREB target genes.

In contrast to i.p. insulin, refeeding for 30 or 90 min attenuated the ChIP signals for all three coactivators (CBP, p300 and CRTC2) at the *Pck1* promoter (Figure 2G), consistent with the reduced expression of *Pck1* in response to refeeding (Figure 2C). This suggests two things: 1) refeeding and insulin injection are not equivalent for disrupting CREB coactivator complex formation and inhibiting transcription; 2) the recruitment of multiple coactivators must be inhibited to repress hepatic gluconeogenic gene expression, which agrees with our results using CBP liver knockout mice.

The Δ CH1 mutation in CBP and p300 removes critical CH1 domain components

Although our data indicates that CBP in the liver is not essential for glucose homeostasis, mice heterozygous for a *CBP* germline mutation that truncates at aa 1084 (deleting 1357 residues) are lean and insulin-sensitive (Yamauchi et al., 2002). The *CBP* functional deficiencies that lead to this phenotype are unclear, however. One clue was provided by a report that the CH1 domain of CBP is important for transactivation in response to insulin (Zanger et al., 2001). In addition, a S436A germline mutation in *CBP* causes an insulin-resistant phenotype (Zhou et al., 2004), suggesting that it is the CH1 domain that is important for metabolic control.

We tested this idea by using mice carrying deletions in one of the two exons that encode the CH1 (TAZ1) domain of CBP (*CBP^{\Delta}CH1*) and p300 (*p300^{\Delta}CH1*) (Kasper et al., 2005). The deletion mutations are essentially equivalent in CBP and p300 (aa 342-393 deleted for CBP, and 329-379 for p300), and remove two of the domain's four α -helices, five Cys and His residues that bind two of the three zinc ions in the structure, 8 of 14 residues that form the conserved hydrophobic core, and much of the binding surface for HIF-1 α and CITED2 (Dames et al., 2002; De Guzman et al., 2004; Freedman et al., 2003; Freedman et al., 2002) (Figures 3A, S3A). The hydrophobic core and binding of zinc are essential for the structural integrity of the CH1 domain (Gu et al., 2001; Matt et al., 2004; Newton et al., 2000), indicating that the Δ CH1 mutation will inhibit the interaction with most, if not all CH1-binding partners. Ser436 is part of the extended CBP CH1 α 4 helix that is not removed by the Δ CH1 mutation (Figures 3A, S3A), although interactions between α 4 and the hydrophobic core of the domain are disrupted by the deletion of helices α 1 and α 2 (De Guzman et al., 2004). Thus, whether the hypoglycemic effects of insulin or metformin require an intact CH1 structure can be addressed using these mice.

Improved glucose tolerance and insulin sensitivity in *CBP^{\Delta}CH1/ Δ CH1* and *p300^{\Delta}CH1/ Δ CH1* mice

We tested whether fasting blood glucose is affected in *CBP^{\Delta}CH1/ Δ CH1* mice but found no significant effect compared to controls ($P > 0.05$, Figure 3B). A similar result was obtained

using $p300^{\Delta CH1/\Delta CH1}$ mice ($P > 0.05$, Figure 3C). In agreement with the fasting glucose results, hepatic gluconeogenic gene expression was not significantly altered in fasted $p300^{\Delta CH1/\Delta CH1}$ and $CBP^{\Delta CH1/\Delta CH1}$ mice (2-3 month-old males, Figures 3D-F; 2-5 month females, Figures 3G-I). Interestingly, some, but not all, 8-10 month male $CBP^{\Delta CH1/\Delta CH1}$ mice showed elevated expression of *G6pc*, *Pck1* and *Ppargc1a* in the liver, although fasting blood glucose was not significantly different from age-matched WT and $p300^{\Delta CH1/\Delta CH1}$ mice (Figures S3B-E). Comparing our results from the different age cohorts suggests that variable gluconeogenic gene expression amongst older $CBP^{\Delta CH1/\Delta CH1}$ mutants reflects an indirect effect of their physiological status rather than a direct action of the CBP $\Delta CH1$ protein on liver target genes. Nonetheless, severe disruption of the CBP or p300 CH1 domain structure in every tissue of the mouse does not affect fasting blood glucose, expanding upon the result obtained with conditional knockout of *CBP* in liver.

We next performed glucose tolerance tests (GTT), as *CBP* S436A mutant mice are glucose intolerant and insulin resistant (Zhou et al., 2004), while mice heterozygous for a truncated allele of CBP (retaining CH1 but lacking the HAT domain) have increased glucose tolerance and insulin responsiveness (Yamauchi et al., 2002). In contrast to *CBP* S436A mutants, $CBP^{\Delta CH1/\Delta CH1}$ and $p300^{\Delta CH1/\Delta CH1}$ mice showed improved glucose tolerance relative to WT animals ($P < 0.05$, Figures 3J,K). Improved glucose tolerance in the $\Delta CH1$ mutants indicates insulin-sensitization, so we performed insulin tolerance tests (ITTs). $CBP^{\Delta CH1/\Delta CH1}$ ($P < 0.05$) and $p300^{\Delta CH1/\Delta CH1}$ ($P < 0.001$) mice both showed an enhanced ability to lower blood glucose in response to insulin, indicating that their improved glucose responsiveness was due to increased insulin sensitivity (Figures 3L,M). As *CBP* liver knockout mice had normal ITT and GTT responses (Figure S1F-I), these results indicate that the CH1 domain of CBP and p300 is critical outside the liver for glucose homeostasis. Speculating, it might be that the *CBP* truncation (Yamauchi et al., 2002) and $\Delta CH1$ mutations similarly affect these physiological functions via related mechanisms (e.g. inhibiting the activity of a CH1-binding transcription factor).

***CBP* ^{$\Delta CH1/\Delta CH1$} mice lower their blood glucose normally in response to the anti-diabetic drug metformin**

The CBP CH1 structural domain could be inferred to mediate the glucose lowering effect of metformin that occurs in response to Ser436 phosphorylation (He et al., 2009). To examine this, we performed metformin tolerance testing (MTTs). This showed that i.p. metformin lowered fasting blood glucose levels similarly in WT and $CBP^{\Delta CH1/\Delta CH1}$ mice ($P > 0.05$) when compared to i.p. saline (Figure 3N). Thus, disrupting the CH1 domain structure of CBP enhances insulin-sensitivity but it does not affect the blood glucose-lowering action of metformin.

***CBP* ^{$\Delta CH1/\Delta CH1$} and *p300* ^{$\Delta CH1/\Delta CH1$} mice have reduced body weight and white adipose tissue**

Increased insulin-responsiveness suggests enhanced metabolic control. In line with this, $CBP^{\Delta CH1/\Delta CH1}$ and $p300^{\Delta CH1/\Delta CH1}$ mice at 4-16 months of age had significantly reduced white adipose tissue (WAT) as percentage of body weight, which became more apparent with age (male data, Figures 4A,B; female data, S4A-C).

Consistent with reduced WAT, $CBP^{\Delta CH1/\Delta CH1}$ mice weighed less than same sex controls at all ages (males, Figures 4C; females, S4D). Although growth retardation of $CBP^{\Delta CH1/\Delta CH1}$ mice accounted for part of their reduced weight, they had a lower body mass index (BMI) than WT mice as early as 4-6 months of age (Figure 4D), indicating that their reduced weight was not solely due to their smaller size. $CBP^{+/\Delta CH1}$ mice showed an intermediate phenotype for body weight and BMI, especially as they aged (Figures 4C,D, S4D).

p300^{ΔCH1/ΔCH1} mice were not growth retarded, yet they also exhibited lower body weight (Figures 4E, males; S4E, females) and reduced BMI (Figure 4D). WT, *CBP^{ΔCH1/ΔCH1}* and *p300^{ΔCH1/ΔCH1}* mice consumed similar amounts of normal chow (not shown), although *CBP^{ΔCH1/ΔCH1}* mutants ate more in comparison to their body weight ($P < 0.05$, Figure 4F). This indicates the reduced BMI of the Δ CH1 mutants is not due to decreased food intake. Thermogenic brown adipose tissue (BAT) might be expected to be more abundant in lean animals, but it was actually reduced in 10-12 month old *CBP^{ΔCH1/ΔCH1}* mice relative to WT, although this difference was not significant when normalized to body weight ($P > 0.05$, Figures S4F,G).

WAT adipocytes from *CBP^{ΔCH1/ΔCH1}* mice are smaller

The reduced WAT mass in Δ CH1 mutant mice could be caused by fewer or smaller fat cells. Histological analysis of gonadal WAT from 4-6 month old *CBP^{ΔCH1/ΔCH1}* mice showed that adipocytes were smaller compared to controls ($P < 0.05$, Figures 4G,H). To help determine if the Δ CH1 mutation inhibits fat synthesis or storage, we differentiated WT and *CBP^{ΔCH1/ΔCH1};p300^{+ΔCH1}* MEFs into adipocytes *ex vivo*. These mutant adipocytes were severely deficient for normal CH1 domains but they did not obviously differ from WT cells as shown by Oil Red-O staining for lipids and the expression of adipogenic marker genes encoding peroxisome proliferator activated receptor gamma (PPAR gamma, *Pparg*), fatty acid synthase (FAS, *Fasn*), and glucose transporter-4 (GLUT4, *Slc2a4*) (Figure 5). Consistent with these *in vitro* findings, expression of the fatty acid storage and metabolism genes *Plin2*, *Fabp4*, *Fabp5*, *Plin1*, *Cpt1b*, and *Acaca* in WAT isolated from 8-10 month old WT, *CBP^{ΔCH1/ΔCH1}* and *p300^{ΔCH1/ΔCH1}* mice was comparable ($P > 0.05$, Figure S5A-F). In addition, fatty acid oxidation measurements (Brivet et al., 1995; Buzzai et al., 2005) using adipocytes isolated from WAT were not obviously different between wild type and mutants when normalized to nuclear DNA, which is indicative of cell number (Figure S5G,H; Figure 4G shows that the mutant adipocytes are smaller and thus more abundant on a tissue weight basis). These results together suggest that reduced WAT mass in Δ CH1 mutant mice is caused by altered energy demand or storage, rather than abnormal adipogenesis or adipocyte fatty acid metabolism.

p300^{ΔCH1/ΔCH1} mice are resistant to the adverse metabolic consequences of a high fat diet

The enhanced metabolic control observed in Δ CH1 mutant mice fed a normal chow diet suggested that they would be more resistant to the deleterious effects of a high fat diet (HFD). We tested this idea using 10-12 month-old *p300^{ΔCH1/ΔCH1}* male mice. At this age, the mutants started out relatively lean, yet after 12 weeks of HFD they still weighed significantly less than HFD WT animals, despite similar food intake (Figures 6A,B). Moreover, *p300^{ΔCH1/ΔCH1}* mice showed resistance to HFD-induced elevated serum triglycerides, glucose intolerance, and insulin resistance when compared to WT controls ($P < 0.05$, Figures 6C-E). Together, these findings suggest that reducing CH1 functionality increases metabolic control with both normal and high fat diets.

DISCUSSION

Using a tissue-specific conditional knockout of *CBP*, we demonstrated that this HAT is not limiting in the liver for glucose homeostasis or hepatic gluconeogenic gene expression. However, germline mutations in *CBP* and *p300* that severely disrupt the structure of CH1 showed that this domain is critical for maintaining fat reserves, although it is not limiting for the blood glucose lowering activities of insulin and metformin. Consistent with their lean phenotype, both *CBP^{ΔCH1/ΔCH1}* and *p300^{ΔCH1/ΔCH1}* mice were insulin sensitized, showing that disrupting the CH1 domain improves metabolic control *in vivo*. And for *CBP* at least, the critical organ system(s) for regulating glucose homeostasis appears to be outside the

liver. Thus, identifying the transcription factor-binding CH1 domain as a key component of a metabolic regulatory pathway provides mechanistic insight into how CBP and p300 modulate energy homeostasis.

The CH1 domain is one of the few regions of a mammalian HAT to have been analyzed *in vivo* using more than one knock-in mutation (i.e. Δ CH1 and S436A mice). Our findings therefore help reveal how this domain controls energy homeostasis, a topic relevant to the expanding roles ascribed to acetyltransferases in metabolism (Feige and Auwerx, 2007; Zhao et al., 2010), and the fact that CBP and p300 act as regulatory network “hubs” (they have more than 400 described protein interaction partners) (Bedford et al., 2010). With regard to CH1-binding partners, hypoxia inducible factor 1 α (HIF-1 α), which requires the CH1 domain for its full transactivation activity (Kasper et al., 2005; Kasper and Brindle, 2006), affects adipose tissue in complex ways (Halberg et al., 2009; Zhang et al., 2010), but the expression of HIF-target genes *Edn1*, *Higd1a*, *Slc2a1* (GLUT1), and *Vegfa* (VEGF) was not repressed in WAT directly isolated from $CBP^{\Delta CH1/\Delta CH1}$ and $p300^{\Delta CH1/\Delta CH1}$ mice (data not shown). Additionally, identifying the CH1 domain as a mediator of the metabolic functions of CBP helps clarify prior findings that implicated CBP in both insulin-sensitized (Yamauchi et al., 2002) and insulin-resistant phenotypes (He et al., 2009). The similar metabolic phenotype we observe with both $CBP^{\Delta CH1/\Delta CH1}$ and $p300^{\Delta CH1/\Delta CH1}$ mice argues that the role for the CH1 domain in energy homeostasis is not specific to only one member of the KAT3 family.

The Δ CH1 mutation does not remove Ser436 in CBP but the differences between the $CBP^{\Delta CH1}$ and S436A phenotypes are not inconsistent if the Δ CH1 mutation acts independently of Ser436 phosphorylation. A role for the CH1 domain in metabolic control that is independent of Ser436 is supported by the similarities of the metabolic phenotypes of $CBP^{\Delta CH1/\Delta CH1}$ and $p300^{\Delta CH1/\Delta CH1}$ mice even though p300 CH1 has a glycine at the position comparable to Ser436. If, for example, Ser436 phosphorylation in response to insulin inhibits CBP CH1 domain function then the Δ CH1 mutation might have mimicked the effect of this phosphorylation and promoted fasting hypoglycemia. We did not see this, however, as $CBP^{\Delta CH1/\Delta CH1}$ mice had normal fasting blood glucose levels, although they did have an enhanced response to injected glucose or insulin. On the other hand, if the Δ CH1 mutation prevents Ser436 phosphorylation, or disrupts the ability of phospho-Ser436 to activate CH1 (or other CBP domains or binding partners), then one might expect $CBP^{\Delta CH1/\Delta CH1}$ mice to be insulin-resistant like S436A mutants, which they are not. Alternatively, the CH1 domain and Ser436 may act by independent physiological pathways. In support of the latter model, the glucose-lowering activity of metformin was not affected by the $CBP^{\Delta CH1}$ mutation, which also suggests that this drug works differently from insulin. It is important to reemphasize, however, that loss of CBP in the liver had no measurable effect on glucose homeostasis, indicating that the phosphorylation of hepatic CBP Ser436 is not physiologically relevant for that function.

Indeed, several of our findings are inconsistent with the model where CBP Ser436 phosphorylation by insulin-stimulated PKC ι/λ inhibits CREB:CBP complex formation at gluconeogenic genes in the liver, thereby reducing gluconeogenesis and blood glucose levels (He et al., 2009; Zhou et al., 2004).

First, in contrast to a fast/refeed paradigm, we did not observe an obvious and sustained decrease in gluconeogenic gene mRNA levels in the livers of fasted wild type mice injected with insulin. Nor did we observe an insulin-dependent loss of CBP recruitment to such genes. It is possible that our failure to observe these phenomena was due to experimental conditions (e.g. mouse strain) or approach (e.g. euglycemia was not maintained). Nevertheless, a reduction in gluconeogenic gene expression would seem unlikely to

contribute substantially to an acute reduction in blood glucose in response to insulin. In this regard, Ramnanan *et al.* have shown that reduced hepatic glucose output in response to acute hyperinsulinemia in euglycemic fasted canines is mostly due to changes in glycolysis and glycogen synthesis rather than the repression of gluconeogenesis via downregulation of *Pck1* expression (Ramnanan *et al.*, 2010).

Second, we showed that conditional knockout of CBP in the liver did not significantly affect fasting blood glucose levels or gluconeogenic gene expression. It is possible that using different methods to reduce liver CBP (e.g. RNAi vs. knockout) might lead to different phenotypes, but the knockout data is consistent with a model where CBP in the liver is not limiting for glucose homeostasis.

Third, we found that PKC iota (PKC_{ι} , $PKC_{\iota/\lambda}$, PKC_{λ}), which is modeled as the insulin-responsive CBP Ser436 kinase in liver (He *et al.*, 2009), does not measurably phosphorylate Ser436 *in vitro*. Using purified recombinant PKC_{ι} (Promega), we did not observe evidence for significant inducible Ser436 phosphorylation with the following substrates: 1) wild type, $\Delta CH1$, S436A, and $\Delta CH1/S436A$ CBP-HA proteins expressed in 293T cells and immunoprecipitated with anti-HA antibody (Figures 7A,B); 2) a synthetic CBP 430-442 peptide (LPLKNASDKRNQQ) (Figure 7C); 3) endogenous CBP immunoprecipitated from extracts prepared from serum starved and insulin treated HepG2 cells (Figure S6A); 4) endogenous CBP immunoprecipitated from liver nuclear extracts prepared from fasted wild type mice (Figure S6B); 5) dual-affinity purified full-length GST-CBP-310-452-FLAG proteins (wild type, $\Delta CH1$, S436A, and $\Delta CH1/S436A$ mutants) produced in *E. coli* (Figures S6C,D). Importantly, in each assay, PKC_{ι} was able to efficiently phosphorylate itself and other substrates (e.g. FLAG-CREB, GST-CREM, CREBtide), but not CBP Ser436. The inability of PKC_{ι} to phosphorylate CBP S436 *in vitro* might be explained by the findings of Fujii *et al.* who showed that Asp at the +1 position relative to Ser strongly disfavors phosphorylation by PKC, consistent with the basophilic nature of this kinase family (Fujii *et al.*, 2004). Together, these results indicate that if CBP Ser436 is phosphorylated in response to insulin, it is probably not by PKC_{ι} . Moreover, Matsumoto *et al.* showed that the conditional knockout of PKC iota (also called PKC lambda) in the liver increases insulin sensitivity, and not *Pck1* and *G6pc* expression, further suggesting this kinase does not repress gluconeogenic genes in the liver by phosphorylating CBP Ser436 (Matsumoto *et al.*, 2003).

The normal fasting blood glucose levels seen in $CBP^{\Delta CH1/\Delta CH1}$ mice agreed well with the unchanged hepatic gluconeogenic gene expression and fasting blood glucose we observed in mice deficient in liver CBP, as well as previously published data on $CBP^{KIX/KIX}$ mice (Koo *et al.*, 2005). This suggests other coactivators in the liver besides CBP provide redundant coactivation function for hepatic gluconeogenesis even though CBP is limiting for the expression of other genes in that organ (e.g. *Ndr1*, *Ppp1c3*). This is consistent with the notion that individual CREB target genes dictate and utilize different coactivator mechanisms for their expression in response to cAMP (Kasper *et al.*, 2010; Xu *et al.*, 2007). p300 is a prime HAT candidate to compensate for the loss of liver CBP, and analysis of CBP and p300 mRNA and protein levels in the liver suggests that the two coactivators are present in comparable amounts (Figures S1P-R) (Thorrez *et al.*, 2008). The non-HAT CRT2 may also provide functional redundancy as it is limiting for the expression of certain CREB-target genes in MEFs (Kasper *et al.*, 2010), and for *Pparg1a*, *Pck1* and *G6pc* in the liver (Le Lay *et al.*, 2009; Wang *et al.*, 2010).

The metabolic functions of the CH1 domain are limiting as mice heterozygous for the $\Delta CH1$ mutation in *CBP* and *p300* tended to have intermediate phenotypes for adiposity and insulin-sensitivity. Moreover, $p300^{\Delta CH1/\Delta CH1}$ mice resisted the weight gain, glucose intolerance and

insulin resistance associated with a high-fat diet. These characteristics of the CH1 domain suggest that it would be a sensitive drug target for increasing metabolic control.

EXPERIMENTAL PROCEDURES

Animals

CBP^{ΔCH1}, *p300^{ΔCH1}* and *CBP^{fllox}* mice were previously described (Kang-Decker et al., 2004; Kasper et al., 2005). All studies used C57BL/6 X 129Sv F1 hybrid mice derived from congenic parents. F1 *p300^{ΔCH1/ΔCH1}* mice were normal in appearance and had body lengths similar to WT animals, whereas adult *CBP^{ΔCH1/ΔCH1}* mice were smaller and had moderate craniofacial anomalies (Kasper et al., 2005) (chiefly, blunt snouts, unpublished data). All mice were used and cared for following protocols approved by the Institutional Animal Care and Use Committee of St. Jude.

Histology

Gonadal WAT pads were fixed with formaldehyde and stained with hematoxylin and eosin. ImageJ software was used to determine the number of cells for each of four random microscope fields of view for each of 4 serial sections cut $\geq 40\mu\text{M}$ apart.

Cell culture

CBP^{ΔCH1/ΔCH1};p300^{+/ΔCH1} primary MEFs were described previously (Kasper et al., 2005). Differentiation of *CBP^{ΔCH1/ΔCH1};p300^{+/ΔCH1}* and WT MEFs into adipocytes was carried out as described (Tanaka et al., 1997a), using Dulbecco's Modified Eagle medium (DMEM) supplemented with 10% heat-inactivated FBS, 0.5 mM IBMX, 1 μM dexamethasone, 5 $\mu\text{g}/\text{ml}$ insulin. This medium was renewed every other day for 12 days.

Metabolic studies

Fasting blood glucose was measured by tail vein bleed and a Glucometer Elite (Bayer). GTT assays were performed on mice after a 16-hour overnight fast. Animals were injected i.p. with 20% D-glucose (2 mg/g body weight) and blood glucose was measured at the indicated times. ITT assays were carried out on mice fasted for 3 hours, injected i.p. with human insulin (0.75 IU/kg) and blood glucose measured at the indicated times. MTT assays were performed on mice fasted for 16 hr and injected i.p. with metformin (250 mg/kg) or saline vehicle. Human recombinant insulin (Humulin N, Lilly) was used as indicated for the animal experiments shown. Hepatic gene expression assays using wild type mice injected with 0.75 IU/kg bovine insulin purchased from Sigma (I5500) yielded comparable results to Humulin N (data not shown).

High Fat Diet assays

10-12 month-old male WT and *p300^{ΔCH1/ΔCH1}* mice were fed a high-fat diet *ad libitum* for 12 weeks (60% kcal from fat; Research Diets, NJ). Body weight and food intake were monitored. GTT and ITT assays were performed (as described above) following 10 and 12 weeks respectively on the HFD. Serum triglycerides were measured using a kit (Sigma Cat# TR0100) and serum from retro-orbital bleeds obtained one-hour post-prandial from anesthetized mice that had been fasted 16 hours overnight.

Cre mediated deletion of *CBP^{fllox}* in liver

Mice were tail-vein injected with 2.5×10^{10} genome copies of AAV-2/8-LP1-Cre (Cre expression driven by the liver-specific promoter of lipoprotein-1). Six days post injection, male *CBP^{fllox/fllox}* mice and WT controls (+/- AAV-Cre, as indicated) were fasted overnight for 16 hr before performing glucose tolerance testing (GTTs). Mice were then assessed for 6

hr fasting blood glucose, and then insulin tolerance testing (ITTs), allowing 72 hr recovery intervals between assays. Finally, 96 hrs following the ITT, mice were fasted overnight for assessment of 16 hr fasting blood glucose and then sacrificed to test hepatic gluconeogenic gene expression. Similar results for 16 hr fasting blood glucose and hepatic gluconeogenic gene expression were obtained seven days after AAV-Cre infection for male and female *CBP^{lox/lox}* mice (Figure S1). All mice within an experiment showed comparable inactivation of *CBP^{lox}* in the liver, as determined by semi-quantitative PCR of genomic DNA (Kasper et al., 2006), qRT-PCR for wild type *CBP* mRNA that contains exon 9 (the exon deleted by Cre-mediated recombination), and IP-western of CBP and p300 using equal volumes of liver nuclear extracts. IP assays performed using pooled rabbit antisera raised against the N- and C-termini of CBP and p300. Western blots were performed using mouse monoclonal antibodies against CBP (C-1) or p300 (RW128).

Quantitative RT-PCR

Real-time reverse-transcription coupled PCR was performed as previously described (Xu et al., 2007). Samples were normalized to β -actin mRNA and the expression levels for each test gene were set relative to the lowest value, which was defined as one.

Liver ChIP

Mice were fasted for 16 hours overnight and after determination of fasting blood glucose were either injected i.p. with 0.5 IU/kg insulin, refed, or sacrificed as fasted controls. Blood glucose was also measured prior to sacrifice of the insulin-treated and refed mice. Whole cell extracts for ChIP were prepared as described (Tuteja et al., 2008) using freshly dissected liver tissue treated for 10 min with 3% formaldehyde, followed by an equal volume of 2.5M glycine. ChIP assays were performed with extracts as described; qPCR ChIP signal was normalized to input chromatin (Kasper et al., 2005).

In vitro kinase assays

In vitro phosphorylation of CBP-HA was carried out (as per manufacturer's instructions) using 5 μ M [³³P]-ATP and 0.1 μ g PKC iota (Promega #V3751), and 293T whole cell extract immunoprecipitates that had been washed sequentially with RIPA buffer (1% Nonidet P-40, 0.5% deoxycholate, 50 mM Tris pH 7.5, 150 mM NaCl), 10 mM Tris pH 7.5/0.1% Nonidet P-40/300mM NaCl, 10 mM Tris pH7.5/0.1% Nonidet P-40/150 mM NaCl, and then 50 mM Tris pH 7.5. Buffers contained protease inhibitors and beta-glycerophosphate. Immunoprecipitations were performed with anti-HA or anti-FLAG monoclonal antibodies and protein G Sepharose. 293T cells were transiently transfected with expression vectors for mouse CBP with an HA C-terminal epitope tag, empty vector, or CREB with a FLAG tag (positive control PKC substrate). IP kinase reactions were incubated with shaking (600 RPM) for 30 min at 30 degrees C. For kinase assays using the synthetic peptides CREBtide (KRREILSRRPSYR, a positive control, Promega) and CBP 430-442 (LPLKNASDKRNQQ), the reactions contained 7.5 μ g peptide (~200 μ M), 50 μ M [³³P]-ATP, and 20 ng PKC iota in 25 μ l and were incubated for 15 min at 30 degrees C. Peptide reactions were terminated by drying 20 μ l onto P81 phosphocellulose paper and then washing 3 times with 1% phosphoric acid.

Statistics

BMI calculated as (weight (kg))/(body length (m))². Data presented as mean \pm standard error of the mean (SEM). Comparisons between groups were made by two-tailed t test or one-way analysis of variance (ANOVA) with Tukey or Dunnett's post-testing. Cumulative effects over time were measured by determining the area under the curve (AUC) using Graphpad Prism. $P > 0.05$ (not significant, N.S.), * $P < 0.05$; ** $P < 0.01$ and *** $P < 0.001$.

Supplementary Material

Refer to Web version on PubMed Central for supplementary material.

Acknowledgments

We thank S. Lerach and T. Jeevan for excellent technical assistance; S. Jackowski, G. Oliver and D. Green for access to equipment; R. Leonard, M. Frank, M Dillard, S. Tait and S. Milasta for providing help and expertise. Thanks to these core facilities at St Jude: Animal Resource Center, Animal Pathology, Biomedical Communications, and Vector Production and Development. The Hartwell Center at St. Jude provided oligonucleotides. This work was supported by NIH grants DK058199 and DE018183 (P.B.), Cancer Center (CORE) support grant P30 CA021765, and the American Lebanese Syrian Associated Charities of St. Jude Children's Research Hospital.

REFERENCES

- Allis CD, Berger SL, Cote J, Dent S, Jenuwien T, Kouzarides T, Pillus L, Reinberg D, Shi Y, Shiekhattar R, Shilatifard A, Workman J, Zhang Y. New nomenclature for chromatin-modifying enzymes. *Cell*. 2007; 131:633–636. [PubMed: 18022353]
- Bedford DC, Kasper LH, Fukuyama T, Brindle PK. Target gene context influences the transcriptional requirement for the KAT3 family of CBP and p300 histone acetyltransferases. *Epigenetics*. 2010; 5:9–15. [PubMed: 20110770]
- Biddinger SB, Kahn CR. From mice to men: insights into the insulin resistance syndromes. *Annual review of physiology*. 2006; 68:123–158.
- Brivet M, Slama A, Saudubray JM, Legrand A, Lemonnier A. Rapid diagnosis of long chain and medium chain fatty acid oxidation disorders using lymphocytes. *Ann Clin Biochem*. 1995; 32(Pt 2): 154–159. [PubMed: 7785942]
- Buzzai M, Bauer DE, Jones RG, Deberardinis RJ, Hatzivassiliou G, Elstrom RL, Thompson CB. The glucose dependence of Akt-transformed cells can be reversed by pharmacologic activation of fatty acid beta-oxidation. *Oncogene*. 2005; 24:4165–4173. [PubMed: 15806154]
- Dames SA, Martinez-Yamout M, De Guzman RN, Dyson HJ, Wright PE. Structural basis for Hif-1 alpha /CBP recognition in the cellular hypoxic response. *Proc Natl Acad Sci U S A*. 2002; 99:5271–5276. [PubMed: 11959977]
- De Guzman RN, Martinez-Yamout MA, Dyson HJ, Wright PE. Interaction of the TAZ1 domain of the CREB-binding protein with the activation domain of CITED2: regulation by competition between intrinsically unstructured ligands for non-identical binding sites. *J Biol Chem*. 2004; 279:3042–3049. [PubMed: 14594809]
- Feige JN, Auwerx J. Transcriptional coregulators in the control of energy homeostasis. *Trends Cell Biol*. 2007; 17:292–301. [PubMed: 17475497]
- Freedman SJ, Sun ZY, Kung AL, France DS, Wagner G, Eck MJ. Structural basis for negative regulation of hypoxia-inducible factor-1alpha by CITED2. *Nat Struct Biol*. 2003; 10:504–512. [PubMed: 12778114]
- Freedman SJ, Sun ZY, Poy F, Kung AL, Livingston DM, Wagner G, Eck MJ. Structural basis for recruitment of CBP/p300 by hypoxia-inducible factor-1 alpha. *Proc Natl Acad Sci U S A*. 2002; 99:5367–5372. [PubMed: 11959990]
- Fujii K, Zhu G, Liu Y, Hallam J, Chen L, Herrero J, Shaw S. Kinase peptide specificity: improved determination and relevance to protein phosphorylation. *Proc Natl Acad Sci U S A*. 2004; 101:13744–13749. [PubMed: 15356339]
- Gu J, Milligan J, Huang LE. Molecular mechanism of hypoxia-inducible factor 1alpha -p300 interaction. A leucine-rich interface regulated by a single cysteine. *J Biol Chem*. 2001; 276:3550–3554. [PubMed: 11063749]
- Halberg N, Khan T, Trujillo ME, Wernstedt-Asterholm I, Attie AD, Sherwani S, Wang ZV, Landskroner-Eiger S, Dineen S, Magalang UJ, Brekken RA, Scherer PE. Hypoxia-inducible factor 1alpha induces fibrosis and insulin resistance in white adipose tissue. *Mol Cell Biol*. 2009; 29:4467–4483. [PubMed: 19546236]

- He L, Sabet A, Djedjos S, Miller R, Sun X, Hussain MA, Radovick S, Wondisford FE. Metformin and insulin suppress hepatic gluconeogenesis through phosphorylation of CREB binding protein. *Cell*. 2009; 137:635–646. [PubMed: 19450513]
- Herzig S, Long F, Jhala US, Hedrick S, Quinn R, Bauer A, Rudolph D, Schutz G, Yoon C, Puigserver P, Spiegelman B, Montminy M. CREB regulates hepatic gluconeogenesis through the coactivator PGC-1. *Nature*. 2001; 413:179–183. [PubMed: 11557984]
- Hirschey MD, Shimazu T, Goetzman E, Jing E, Schwer B, Lombard DB, Grueter CA, Harris C, Biddinger S, Ilkayeva OR, Stevens RD, Li Y, Saha AK, Ruderman NB, Bain JR, Newgard CB, Farese RV Jr, Alt FW, Kahn CR, Verdin E. SIRT3 regulates mitochondrial fatty-acid oxidation by reversible enzyme deacetylation. *Nature*. 2010; 464:121–125. [PubMed: 20203611]
- Kang-Decker N, Tong C, Boussouar F, Baker DJ, Xu W, Leontovich AA, Taylor WR, Brindle PK, Van Deursen JM. Loss of CBP causes T cell lymphomagenesis in synergy with p27(Kip1) insufficiency. *Cancer Cell*. 2004; 5:177–189. [PubMed: 14998493]
- Kasper LH, Boussouar F, Boyd K, Xu W, Biesen M, Rehg J, Baudino TA, Cleveland JL, Brindle PK. Two transactivation mechanisms cooperate for the bulk of HIF-1-responsive gene expression. *Embo J*. 2005; 24:3846–3858. [PubMed: 16237459]
- Kasper LH, Boussouar F, Ney PA, Jackson CW, Rehg J, van Deursen JM, Brindle PK. A transcription-factor-binding surface of coactivator p300 is required for haematopoiesis. *Nature*. 2002; 419:738–743. [PubMed: 12384703]
- Kasper LH, Brindle PK. Mammalian gene expression program resiliency: the roles of multiple coactivator mechanisms in hypoxia-responsive transcription. *Cell Cycle*. 2006; 5:142–146. [PubMed: 16357535]
- Kasper LH, Fukuyama T, Biesen MA, Boussouar F, Tong C, de Pauw A, Murray PJ, van Deursen JM, Brindle PK. Conditional knockout mice reveal distinct functions for the global transcriptional coactivators CBP and p300 in T-cell development. *Mol Cell Biol*. 2006; 26:789–809. [PubMed: 16428436]
- Kasper LH, Lerach S, Wang J, Wu S, Jeevan T, Brindle PK. CBP/p300 double null cells reveal effect of coactivator level and diversity on CREB transactivation. *Embo J*. 2010; 29:3660–3672. [PubMed: 20859256]
- Koo SH, Flechner L, Qi L, Zhang X, Srean RA, Jeffries S, Hedrick S, Xu W, Boussouar F, Brindle P, Takemori H, Montminy M. The CREB coactivator TORC2 is a key regulator of fasting glucose metabolism. *Nature*. 2005; 437:1109–1114. [PubMed: 16148943]
- Kung AL, Rebel VI, Bronson RT, Ch'ng LE, Sieff CA, Livingston DM, Yao TP. Gene dose-dependent control of hematopoiesis and hematologic tumor suppression by CBP. *Genes Dev*. 2000; 14:272–277. [PubMed: 10673499]
- Le Lay J, Tuteja G, White P, Dhir R, Ahima R, Kaestner KH. CRTC2 (TORC2) contributes to the transcriptional response to fasting in the liver but is not required for the maintenance of glucose homeostasis. *Cell Metab*. 2009; 10:55–62. [PubMed: 19583954]
- Lipina C, Huang X, Finlay D, McManus EJ, Alessi DR, Sutherland C. Analysis of hepatic gene transcription in mice expressing insulin-insensitive GSK3. *Biochem J*. 2005; 392:633–639. [PubMed: 16176184]
- Marmorstein R. Structure of histone acetyltransferases. *J Mol Biol*. 2001; 311:433–444. [PubMed: 11492997]
- Matsumoto M, Ogawa W, Akimoto K, Inoue H, Miyake K, Furukawa K, Hayashi Y, Iguchi H, Matsuki Y, Hiramatsu R, Shimano H, Yamada N, Ohno S, Kasuga M, Noda T. PKC λ in liver mediates insulin-induced SREBP-1c expression and determines both hepatic lipid content and overall insulin sensitivity. *J Clin Invest*. 2003; 112:935–944. [PubMed: 12975478]
- Matt T, Martinez-Yamout MA, Dyson HJ, Wright PE. The CBP/p300 TAZ1 domain in its native state is not a binding partner of MDM2. *Biochem J*. 2004; 381:685–691. [PubMed: 15154850]
- Newton AL, Sharpe BK, Kwan A, Mackay JP, Crossley M. The transactivation domain within cysteine/histidine-rich region 1 of CBP comprises two novel zinc-binding modules. *J Biol Chem*. 2000; 275:15128–15134. [PubMed: 10748221]
- Oike Y, Hata A, Mamiya T, Kaname T, Noda Y, Suzuki M, Yasue H, Nabeshima T, Araki K, Yamamura K. Truncated CBP protein leads to classical Rubinstein-Taybi syndrome phenotypes in

- mice: implications for a dominant-negative mechanism. *Hum.Mol.Genet.* 1999; 8:387–396. [PubMed: 9949198]
- Ramnanan CJ, Edgerton DS, Rivera N, Irimia-Dominguez J, Farmer B, Neal DW, Lautz M, Donahue EP, Meyer CM, Roach PJ, Cherrington AD. Molecular characterization of insulin-mediated suppression of hepatic glucose production in vivo. *Diabetes.* 2010; 59:1302–1311. [PubMed: 20185816]
- Tanaka T, Yoshida N, Kishimoto T, Akira S. Defective adipocyte differentiation in mice lacking the C/EBPbeta and/or C/EBPdelta gene. *Embo J.* 1997a; 16:7432–7443. [PubMed: 9405372]
- Tanaka Y, Naruse I, Maekawa T, Masuya H, Shiroishi T, Ishii S. Abnormal skeletal patterning in embryos lacking a single Cbp allele: a partial similarity with Rubinstein-Taybi syndrome. *Proc Natl Acad Sci U S A.* 1997b; 94:10215–10220. [PubMed: 9294190]
- Thorrez L, Van Deun K, Tranchevent LC, Van Lommel L, Engelen K, Marchal K, Moreau Y, Van Mechelen I, Schuit F. Using ribosomal protein genes as reference: a tale of caution. *PLoS ONE.* 2008; 3:e1854. [PubMed: 18365009]
- Tilghman SM, Hanson RW, Reshef L, Hoppgood MF, Ballard FJ. Rapid loss of translatable messenger RNA of phosphoenolpyruvate carboxykinase during glucose repression in liver. *Proc Natl Acad Sci U S A.* 1974; 71:1304–1308. [PubMed: 4364533]
- Tuteja G, Jensen ST, White P, Kaestner KH. Cis-regulatory modules in the mammalian liver: composition depends on strength of Foxa2 consensus site. *Nucleic Acids Res.* 2008; 36:4149–4157. [PubMed: 18556755]
- Wang Y, Inoue H, Ravnskjaer K, Viste K, Miller N, Liu Y, Hedrick S, Vera L, Montminy M. Targeted disruption of the CREB coactivator Crtc2 increases insulin sensitivity. *Proc Natl Acad Sci U S A.* 2010; 107:3087–3092. [PubMed: 20133702]
- Xu W, Kasper LH, Lerach S, Jeevan T, Brindle PK. Individual CREB-target genes dictate usage of distinct cAMP-responsive coactivation mechanisms. *Embo J.* 2007; 26:2890–2903. [PubMed: 17525731]
- Yamauchi T, Oike Y, Kamon J, Waki H, Komeda K, Tsuchida A, Date Y, Li MX, Miki H, Akanuma Y, Nagai R, Kimura S, Saheki T, Nakazato M, Naitoh T, Yamamura K, Kadowaki T. Increased insulin sensitivity despite lipodystrophy in Crebbp heterozygous mice. *Nat Genet.* 2002; 30:221–226. [PubMed: 11818964]
- Yao TP, Oh SP, Fuchs M, Zhou ND, Ch'ng LE, Newsome D, Bronson RT, Li E, Livingston DM, Eckner R. Gene dosage-dependent embryonic development and proliferation defects in mice lacking the transcriptional integrator p300. *Cell.* 1998; 93:361–372. [PubMed: 9590171]
- Yu J, Auwerx J. The role of sirtuins in the control of metabolic homeostasis. *Ann N Y Acad Sci.* 2009; 1173(Suppl 1):E10–19. [PubMed: 19751409]
- Zanger K, Radovick S, Wondisford FE. CREB Binding Protein Recruitment to the Transcription Complex Requires Growth Factor-Dependent Phosphorylation of Its GF Box. *Mol Cell.* 2001; 7:551–558. [PubMed: 11463380]
- Zhang X, Lam KS, Ye H, Chung SK, Zhou M, Wang Y, Xu A. Adipose tissue-specific inhibition of hypoxia inducible factor 1{alpha} induces obesity and glucose intolerance by impeding energy expenditure in mice. *J Biol Chem.* 2010
- Zhao S, Xu W, Jiang W, Yu W, Lin Y, Zhang T, Yao J, Zhou L, Zeng Y, Li H, Li Y, Shi J, An W, Hancock SM, He F, Qin L, Chin J, Yang P, Chen X, Lei Q, Xiong Y, Guan KL. Regulation of cellular metabolism by protein lysine acetylation. *Science.* 2010; 327:1000–1004. [PubMed: 20167786]
- Zhou XY, Shibusawa N, Naik K, Porras D, Temple K, Ou H, Kaihara K, Roe MW, Brady MJ, Wondisford FE. Insulin regulation of hepatic gluconeogenesis through phosphorylation of CREB-binding protein. *Nat Med.* 2004; 10:633–637. [PubMed: 15146178]

Highlights

- Conditional knockout of CBP in the liver does not affect glucose homeostasis
- Deletion mutation in the CBP or p300 CH1 domain enhances metabolic control
- The CH1 domain is likely critical outside the liver for glucose homeostasis
- CBP CH1 domain mutant mice respond normally to metformin

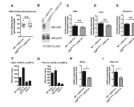


Figure 1. CBP in the liver is not limiting for normal fasting blood glucose and gluconeogenic gene expression

(A) 16 hr fasting blood glucose in 5 month-old WT and *CBP^{flox/flox}* male mice seven days after injection with 2.5×10^{10} g.c. AAV-Cre (WT + AAV-Cre ($N=10$) and *CBP^{flox/flox}* + AAV-Cre ($N=9$)). (B) IP-western of CBP and p300 using liver nuclear extracts. (C-E) qRT-PCR analysis of mRNA for the indicated hepatic gluconeogenic genes after 16 hr fast (WT + AAV-Cre ($N=10$) and *CBP^{flox/flox}* + AAV-Cre ($N=9$)). (F,G) Affymetrix microarray expression signal for the indicated probe sets of *Ndr^{g1}* and *Ppp1r3c* based on mRNA from two independent primary MEF isolates of each genotype [(WT and *CBP* and *p300* double null (dKO)]; serum starved MEFs were treated for 90 min with ethanol vehicle (EtOH) or cAMP agonists forskolin + IBMX (FI), $N=2$. (H,I) *Ndr^{g1}* and *Ppp1r3c* expression in the livers of WT + AAV-Cre ($N=10$) and *CBP^{flox/flox}* + AAV-Cre ($N=9$) fasted male mice. Mean \pm SEM. See also Figure S1.

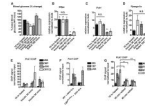


Figure 2. Insulin injection in fasted wild type mice does not rapidly inhibit the CREB:CBP complex or expression of gluconeogenic genes in liver

(A) Compared to fasted WT male mice ($N=23$), refeeding for 90' ($N=4$) and 180' ($N=4$) increases blood glucose, whereas insulin (0.5 IU/kg) rapidly lowers blood glucose 30' ($N=14$), 90' ($N=21$) and 180' ($N=8$) after i.p. injection; (B-D) fasted ($N=8$), insulin-treated ($N=8$ for each time point) or refed ($N=4$ for each time point) WT mice assayed for hepatic gluconeogenic gene expression; one way ANOVA with Dunnett's post test to compare each treatment to untreated fasted mice. (E) ChIP of indicated CREB coactivators at *Pck1* in the livers of fasted WT mice ($N=7$ per indicated treatment); normal rabbit serum control (NRS). (F) CBP and p300 ChIP using livers from fasted mice injected with AAV-Cre ($N=6$). (G) ChIP of CBP, p300 and CRTC2 at *Pck1* in the livers of fasted and refed WT mice; significance of refed versus fasted for the indicated coactivator determined by ANOVA with Tukey post test ($N=7$ mice per indicated treatment). Mean \pm SEM. See also Figure S2.

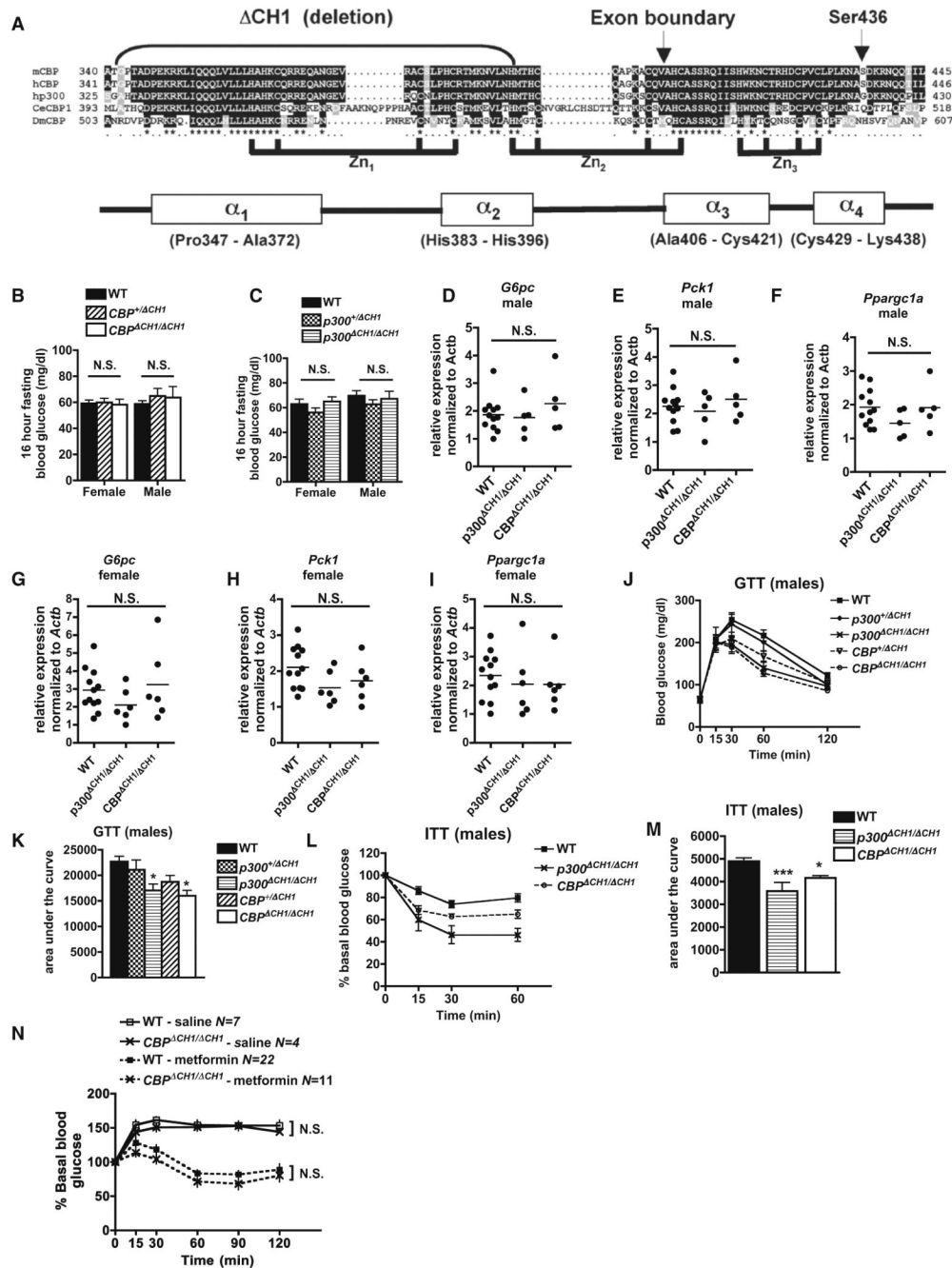


Figure 3. *CBP^{ΔCH1/ΔCH1}* and *p300^{ΔCH1/ΔCH1}* mice have normal fasting blood glucose levels but improved metabolic control

(A) CH1 region deleted in *CBP^{ΔCH1}* and *p300^{ΔCH1}*. Key domain elements indicated: α -helices-1-4 and 12 residues that bind three Zn^{2+} ions; mouse (m), human (h), worm (Ce), fly (Dm). (B,C) 16 hr fasting blood glucose in *CBP^{ΔCH1/ΔCH1}* and *p300^{ΔCH1/ΔCH1}* mice and controls [(B) male WT ($N=18$), *CBP^{+ΔCH1}* ($N=14$), *CBP^{ΔCH1/ΔCH1}* ($N=7$); female WT ($N=14$), *CBP^{+ΔCH1}* ($N=11$), *CBP^{ΔCH1/ΔCH1}* ($N=11$) and (C) male WT ($N=13$), *p300^{+ΔCH1}* ($N=12$), *p300^{ΔCH1/ΔCH1}* ($N=10$); female WT ($N=15$), *p300^{+ΔCH1}* ($N=9$), *p300^{ΔCH1/ΔCH1}* ($N=12$)]. (D-I) qRT-PCR analysis of mRNA for the indicated hepatic gluconeogenic genes after 16 hr fast for 2-3 month-old males (D-F), and 2-5 month females (G-I); each dot

represents a biological replicate, mean value indicated. **(J)** Glucose tolerance test (GTT) for indicated male Δ CH1 mutants and controls; WT ($N=31$), $p300^{+/}\Delta$ CH1 ($N=12$), $p300^{\Delta}$ CH1/ Δ CH1 ($N=10$), CBP^{+}/Δ CH1 ($N=19$), CBP^{Δ} CH1/ Δ CH1 ($N=9$). **(K)** Area under the curve analysis of GTT data shown in (J). **(L)** Insulin tolerance test (ITT) of WT ($N=28$), CBP^{Δ} CH1/ Δ CH1 ($N=9$) and $p300^{\Delta}$ CH1/ Δ CH1 ($N=8$) mice. **(M)** Area under the curve analysis of ITT data shown in (L). **(N)** Metformin tolerance test (MTT) for WT and CBP^{Δ} CH1/ Δ CH1 mice at 4-6 months of age; sample sizes indicated. Fasting blood glucose and GTT analyses performed at 15 weeks of age and ITTs at 6-8 months of age. Mean \pm SEM. See also Figure S3.

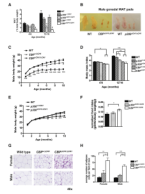


Figure 4. *CBP Δ CH1/ Δ CH1* and *p300 Δ CH1/ Δ CH1* mice have reduced WAT and body mass (A) Male WAT as a percentage of total body weight for genotypes and ages indicated, ($N=5-21$). (B) Male gonadal WAT pads at 12 months of age (right and left pads shown). (C) Body weight profiles for male *CBP Δ CH1* mice (at least 7 mice per genotype). (D) Body mass index (BMI) for male *CBP Δ CH1/ Δ CH1* and *p300 Δ CH1/ Δ CH1* mice at indicated ages ($N=5-19$). (E) Body weight profiles for male *p300 Δ CH1* mice (at least 10 mice per genotype). (F) Average daily food intake normalized to total body weight for WT ($N=18$), *p300 Δ CH1/ Δ CH1* ($N=7$) and *CBP Δ CH1/ Δ CH1* ($N=9$) male mice at 4-8 months of age. (G) H&E stain of gonadal WAT pads. (H) Quantification of average number of cells per field of view in WAT pad sections WT ($N=3$), *CBP $^{+/\Delta}$ CH1* ($N=4$), *CBP Δ CH1/ Δ CH1* ($N=3$). Mean \pm SEM. See also Figure S4.

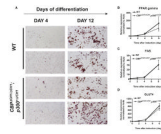


Figure 5. $CBP^{\Delta CH1/\Delta CH1};p300^{+/ \Delta CH1}$ and WT MEFs differentiate comparably into adipocytes (A) Oil Red-O staining of wild type and $CBP^{\Delta CH1/\Delta CH1};p300^{+/ \Delta CH1}$ MEFs cultured for 4 or 12 days in adipocyte-differentiation media. Two independent primary MEF isolates of each genotype shown. (B-D) mRNA levels of adipogenic gene markers PPAR-gamma (*Pparg*), fatty acid synthase (FAS, *Fasn*) and glucose transporter 4 (GLUT4, *Slc2a4*) during the first 8 days of differentiation. $N=2$ independent MEF isolates per genotype. Mean \pm SEM. See also Figure S5.

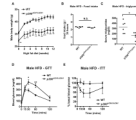


Figure 6. $p300^{ACH1/\Delta CH1}$ mice on a high fat diet have improved serum triglycerides, glucose tolerance and insulin sensitivity compared to WT littermates
(A) Body weights of 10-12 month-old WT ($N=6$) and $p300^{ACH1/\Delta CH1}$ ($N=5$) male mice on a HFD for 12 weeks. **(B)** Food intake between HFD weeks 11 and 12. **(C)** Serum triglyceride levels of male mice fed the HFD for 12 weeks. **(D)** Glucose tolerance test (GTT) data obtained for WT ($N=5$) and $p300^{ACH1/\Delta CH1}$ ($N=5$) after 10 weeks on the HFD. **(E)** Insulin tolerance test (ITT) data for WT ($N=6$) and $p300^{ACH1/\Delta CH1}$ ($N=3$) mice after 12 weeks of HFD. Mean \pm SEM.

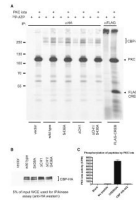


Figure 7. Purified recombinant PKC iota does not efficiently phosphorylate CBP Ser436 *in vitro* (A) SDS PAGE autoradiogram following an *in vitro* kinase assay using 5 μ M [33 P]-ATP, 0.1 μ g PKC iota (indicated) and 293T whole cell extract immunoprecipitates performed with anti-HA or anti-FLAG monoclonal antibodies. 293T cells were transiently transfected with the indicated expression vectors for CBP with an HA C-terminal epitope tag, empty vector, or CREB with a FLAG tag (positive control PKC substrate). The lower two bands of CBP-HA appear to lack the N-terminal region that includes the CH1 domain. Autophosphorylated PKC iota indicated. (B) Western blot with anti-HA antibody shows 5% of input 293T extract used for IP kinase assay. (C) *In vitro* kinase assays using synthetic peptides CREBtide, CBP 430-442, or water (no peptide). Data (c.p.m.) from two independent experiments ($N=2-3$), mean \pm SEM). See also Figure S6.